

Sensor-Actuator Placement for Flexible Structures with Actuator Dynamics

P. G. Maghami* and S. M. Joshi†
NASA Langley Research Center, Hampton, Virginia 23681

A novel approach for placement of sensors and actuators in control of flexible space structures is developed. Using an approximation of the control forces and output measurements by spatially continuous functions, the approach follows a nonlinear programming technique to determine optimal locations for sensors and actuators. Two different criteria are considered for the placement of sensors and actuators. The first criterion optimizes the location of the sensors and actuators in order to move the transmission zeros of the system farther to the left of the imaginary axis. The second criterion, however, places the sensors and actuators to optimize a function of the singular values of the Hankel matrix, which includes both measures of controllability and observability. Moreover, the effect of actuator dynamics in the placement of sensors and actuators is investigated.

Introduction

SENSOR and actuator placement is an integral part of a control design, particularly in the control of flexible structures. Although engineering judgment and trial-and-error analysis are quite often used to determine the optimal locations of sensors and actuators, there have been various attempts to develop systematic means of achieving it. Among a few of these, Chen and Seinfeld¹ used an optimization-based approach wherein optimal locations of measurement outputs are computed from a finite set of possible locations with the aid of integer programming. Skelton and Chiu² have considered an order reduction approach such that the inputs and outputs are reduced from a large set so as to make the smallest possible perturbation in a performance metric. Horta and Juang³ proposed a sequential linear programming approach for truss structures in which optimal numbers as well as locations of actuators are obtained from a large set of actuators. A common point of reference in most of these approaches is the use of a performance metric. To date, various measures of controllability and observability,^{4–5,7} controllability and spillover,⁶ and energy-based metrics² have been considered as performance metrics in the literature. Of recent efforts, Maghami and Joshi⁸ provide a method in which the discrete nature of the sensor and actuator placement problem is transformed into a continuous nonlinear programming problem with the aid of functional approximation of the control forces and output measurements. Lim⁹ proposes an approach for placing actuators and sensors that is based on projecting eigenvectors into the intersection subspace of the controllability and observability subspaces for each sensor-actuator pair.

In this paper, a new approach for sensor and actuator placement in the control of flexible space structures is developed. The approach follows the development of Ref. 8, which reduces the problem of sensor-actuator positioning to a solution of a nonlinear programming optimization. The discrete control forces and output measurements are approximated by spatially continuous functions in order to avoid the discontinuity problems caused when actuators and sensors are recon-

figured within the structure. The structure is then divided into several sections, each allocated with a fixed number of sensors and actuators. With the location of the sensors and actuators within each section as the design variables, a nonlinear programming problem is posed to minimize a performance metric. The main advantage of posing the sensor-actuator placement problem as a nonlinear programming problem is that in this form the placement problem may easily be integrated with other parts of the overall design process, such as control and structural designs. Furthermore, with this formulation, the placement problem may easily be implemented within the integrated controls-structures design process. Here, two different criteria are chosen for the performance metric. In the first criterion, the performance metric is chosen as a function of the finite transmission zeros of the system such that, when optimized, the transmission zeros are moved farther to the left of the imaginary axis. This is a viable choice in view of the asymptotic trend of the closed-loop poles toward the transmission zeros of the system under high gains in fast regulation and tracking problems, as well as in low authority controllers.^{10–12} It also avoids bad transient dynamic characteristics of non-minimum phase systems. In the second criterion, a performance metric related to the singular values of the Hankel matrix is chosen. The optimization then places the sensors and actuators such that the singular values of the Hankel matrix increase in value. Note that the Hankel matrix is the controllability and observability grammians in the balanced realization. The fact that this criterion includes both measures of controllability and observability is quite appealing, since it allows for equal and joint consideration of controllability and observability in placing sensors and actuators, as well as accommodates situations in which some or all of the sensor-actuator pairs are collocated. The effect of actuator dynamics in the placement of sensors and actuators is also considered. It is shown that actuator dynamics can have substantial effects on the optimal locations of sensors and actuators as the actuator bandwidth approaches the operational closed-loop bandwidth. The two criteria are applied to the sensor-actuator placement of a large-order generic space platform.

Analytical Model

The mathematical model of a linear, time-invariant flexible space structure is given by

$$M\ddot{x} + D\dot{x} + Kx = \bar{B}u \quad (1)$$

$$y_p = \bar{C}_p x, \quad y_r = \bar{C}_r \dot{x} \quad (2)$$

where x is an $n \times 1$ displacement vector, M is the positive definite inertia matrix, D is the open-loop damping matrix,

Received July 17, 1991; presented as Paper 91-2606 at the AIAA Guidance, Navigation, and Control Conference, New Orleans, LA, Aug. 12–14, 1991; revision received May 1, 1992; accepted for publication May 28, 1992. Copyright © 1992 by the American Institute of Aeronautics and Astronautics, Inc. No copyright is asserted in the United States under Title 17, U.S. Code. The U.S. Government has a royalty-free license to exercise all rights under the copyright claimed herein for Governmental purposes. All other rights are reserved by the copyright owner.

*Senior Research Engineer, Mail Stop 230.

†Senior Research Scientist, Mail Stop 230.

K is the nonnegative definite stiffness matrix, \bar{B} is an $n \times m$ control influence matrix, u is an $m \times 1$ control input vector, y_p and y_r are, respectively, $p \times 1$ displacement and rate measurements, and \bar{C}_p and \bar{C}_r are the corresponding output influence matrices. Since the order of a large flexible space structure can be quite large, for design and analysis purposes the order of the system is reduced to a design size using model-reduction techniques to obtain

$$M_r \ddot{q}_r + D_r \dot{q}_r + K_r q_r = \Phi^T \bar{B} u \equiv \Gamma^T u \quad (3)$$

$$y_p = \Gamma_p q_r, \quad y_r = \Gamma_r \dot{q}_r \quad (4)$$

where q_r is an $r \times 1$ vector of modal amplitudes; M_r , D_r , K_r are, respectively, the generalized inertia, damping, and stiffness matrices; and Φ is an $n \times r$ matrix whose columns are the r open-loop eigenvectors associated with the included modes. The matrices Γ_p and Γ_r are output influence matrices in modal coordinates. If the mode shapes are normalized with respect to the inertia matrix, and modal damping is assumed, then $M_r = I_{r \times r}$, $D_r = \text{diag}\{2\zeta_1 \omega_1, \dots, 2\zeta_r \omega_r\}$, and $K_r = \text{diag}\{\omega_1^2, \dots, \omega_r^2\}$, where ω_i and ζ_i , $i = 1, \dots, r$, are the open-loop frequencies and damping ratios.

Defining the state vector z

$$z = \{q_r \quad \dot{q}_r\}^T \quad (5)$$

the dynamics of the system can be written in a first-order form

$$\dot{z} = \bar{A}z + \bar{B}u \quad (6)$$

where

$$\bar{A} = \begin{bmatrix} 0 & I_{r \times r} \\ -K_r & -D_r \end{bmatrix}, \quad \bar{B} = \begin{bmatrix} 0 \\ \Gamma^T \end{bmatrix}$$

$$y_p = [\Gamma_p \quad 0]z \equiv \bar{C}_p z, \quad y_r = [0 \quad \Gamma_r]z \equiv \bar{C}_r z$$

The linear dynamics of the actuators can be represented by a first-order time-invariant system, i.e.,

$$\dot{w} = A_a w + B_a v \quad (7a)$$

$$u = C_a w \quad (7b)$$

where A_a , B_a , and C_a are the actuator state, input influence, and output influence matrices, respectively. The vectors v and u represent the desired and applied control forces. Combining Eqs. (6) and (7), one obtains the dynamic equations for a structure with actuator dynamics.

$$\begin{pmatrix} \dot{z} \\ \dot{w} \end{pmatrix} = \begin{bmatrix} \bar{A} & \bar{B}C_a \\ 0 & A_a \end{bmatrix} \begin{pmatrix} z \\ w \end{pmatrix} + \begin{bmatrix} 0 \\ B_a \end{bmatrix} v$$

or in a compact matrix form

$$\dot{\gamma} = A\gamma + Bv \quad (8a)$$

$$y_p = [\bar{C}_p \quad 0]\gamma \equiv C_p \gamma, \quad y_r = [\bar{C}_r \quad 0]\gamma \equiv C_r \gamma \quad (8b)$$

Control Force and Measurement Approximations

Traditionally, the discrete nature of the actuator forces results in certain discontinuities in the optimization process as the actuators are moved along the flexible space structure. These discontinuities are attributed to the nature of force distribution in finite element modeling and can hamper the optimization effort. To avoid such problems, it is feasible to approximate the actuator point forces with spatially continuous functions. For example, if the force in actuator i located at position a_i is equal to f_i , then the actuator force f_i is approximated by the area under the distribution¹³

$$u_i = u_i(x) = \sqrt{\alpha/\pi} f_i e^{-\alpha(x-a_i)^2} \quad (9)$$

where α is a positive scalar that controls the dispersion of the distribution. It can be shown that the total area under the force distribution is equal to f_i , i.e.,

$$\int_{-\infty}^{+\infty} u_i(x) dx = \int_{-\infty}^{+\infty} \sqrt{\alpha/\pi} f_i e^{-\alpha(x-a_i)^2} dx = f_i \quad (10)$$

Furthermore, as $\alpha \rightarrow \infty$ the distribution approaches a Dirac-delta function (a point force). The contribution of the actuator force distribution to each node of the structure depends on the distance of the node to the position of the actuator, as well as to the relative location of the actuator within the bay. The procedure for the computation of nodal forces due to actuator i for a typical truss section shown in Fig. 1 is as follows:

1) Define a local reference point r_i with the global coordinates x_{r_i} , y_{r_i} , z_{r_i} , and a unit direction vector $\bar{\ell}_i$ to define the desired direction for the movement of the actuator. The components of the vector $\bar{\ell}_i$ in the global coordinate system are the cosines of the angles between $\bar{\ell}_i$ and the global XYZ axes, i.e.,

$$\bar{\ell}_i = \cos(\theta_{x_i}) \bar{i} + \cos(\theta_{y_i}) \bar{j} + \cos(\theta_{z_i}) \bar{k} \quad (11)$$

2) With the local x_i axis defined in the direction of vector $\bar{\ell}_i$, compute the area under the actuator force distribution for each bay of the truss structure. As an example, A_j , the area of the force distribution under bay number j , which includes a node N_j with coordinates x_{N_j} , y_{N_j} , z_{N_j} , may be written as

$$A_j = \int_0^{\ell_{\text{Bay}}} \sqrt{\alpha/\pi} f_i \exp\left\{[(x_{N_j} - x_{r_i}) \bar{i} + (y_{N_j} - y_{r_i}) \bar{j} + (z_{N_j} - z_{r_i}) \bar{k}] \cdot \bar{\ell}_i + x_i - a_i\right\}^2 dx_i \quad (12)$$

in which ℓ_{Bay} denotes the length of a bay. Generally, for moderately large values of α in Eq. (9), only the bays in the vicinity of the actuator have appreciable forces. Having obtained the area under the force distributions in each bay, the nodal forces are then obtained using a linear procedure wherein the force distribution on each bay is divided linearly among the nodes of the bay according to their position relative to the centroid of the distribution over the bay. This procedure is straightforward and, hence, is not discussed herein. If the value of f_i , $i = 1, \dots, n_a$ (n_a denotes the number of sensor/actuator pairs) in Eq. (12) is set equal to 1, then the nodal forces obtained in the preceding steps correspond to the elements of the control influence matrix B of Eq. (8).

The same procedure may be followed to approximate the output measurements of the sensors and the elements of the output influence matrices C_p and C_r except that a distribution is used to approximate the measurement instead of force at the sensor location.

To summarize, this approach approximates the actuator forces and output measurements with spatially continuous functions in order to obtain a well-posed optimization with the location of sensors and actuators as design variables.

Transmission Zeros of Flexible Structures

Transmission zeros of linear systems such as the one represented by Eq. (8) are defined as those complex numbers z_i for which there exists a complex vector g_i such that an input of the form $g_i e^{z_i t}$ would result in identically zero output response (with appropriate initial conditions).¹² Denoting the transfer function matrix of the system from the input u to the displacement output y_p by $T(s)$:

$$T(s) = C_p [sI - A]^{-1} B \quad (13)$$

Then, for a transmission zero at z_i , one has

$$T(z_i) g_i e^{z_i t} = C_p [z_i I - A]^{-1} B g_i e^{z_i t} = 0 \quad (14)$$

Moreover, if the triple (A, B, C_p) form an irreducible realization, i.e., the system is fully controllable and observable, then

the transmission zeros are those complex numbers z_i at which the rank of matrix $S(s)$ is reduced.

$$S(s) = \begin{bmatrix} sI - A & -B \\ C_p & 0 \end{bmatrix} \quad (15)$$

Among the attractive properties of transmission zeros is that they are invariant to linear state feedback, which makes them quite important in regulation and tracking problems, as well as low authority controllers, i.e., collocated rate feedback controllers. It has been shown that for such problems the transmission zeros define the asymptotic location of the closed-loop poles under high control gains when the number of inputs and outputs are equal.¹⁰⁻¹² In particular, in linear optimal regulator problems as the weighting on the control effort approaches zero, in order to achieve fast regulation of the output, n_z of the closed-loop poles approach the finite zeros of the open-loop system while the remaining $(2n - n_z)$ poles approach infinity in groups of Butterworth configurations of different orders and radii.^{10,11} It is noted that if the number of sensors and actuators are not equal, then the asymptotic location of the closed-loop poles, as the gains are increased, is defined by the zeros of an augmented system whose state, input influence, and output influence matrices are functions of the triple (A, B, C_p) .¹⁴ It therefore appears that fast regulation is basically possible if the transmission zeros of the system are far enough into the left-half plane. These properties demonstrate the importance of transmission zeros in the control design of linear systems. Linear state feedback does not affect the transmission zeros of the system, but the number and location of the sensors and actuators have a direct impact on their location. Hence, an optimization problem with an objective to move the transmission zeros of the system as far into the left-half plane as possible in order to obtain an optimal location for the sensors and actuators can be a feasible approach to sensor-actuator placement. Here, assume that m sensors, collocated with the actuators, are used to provide output displacement measurements. The collocation of the sensors and actuators will guarantee the system to be minimum phase, i.e., all transmission zeros are in the left-half plane and will enhance the stability robustness of the overall system. This assumption would not effect the generality of this development, since if the sensors and actuators are not collocated (in the sense that the numbers of sensors and actuators are not equal) one would use the transmission zeros of an augmented system (discussed in Ref. 14), rather than the transmission zeros of the system represented by the triple (A, B, C_p) .

Finally, it is appropriate to discuss means of computing the transmission zeros of the system. For a square system presented in Eq. (13), both the finite and infinite transmission zeros may be directly obtained from the solution of the generalized eigenvalue problem

$$\begin{bmatrix} A & -B \\ C_p & 0 \end{bmatrix} \chi = s \begin{bmatrix} I & 0 \\ 0 & 0 \end{bmatrix} \chi \quad (16)$$

Alternatively, a general purpose algorithm by Emami-Naeini and Van Dooren¹⁵ may be used, wherein a reduced-order generalized eigenvalue problem is generated and solved for the finite transmission zeros. A method by Williams¹⁶ that takes advantage of the symmetry and sparsity of the second-order system matrices is also available.

Balanced Realization

Controllability and observability have often been used as measures of effectiveness of actuators and sensors. To date, various measures of controllability and observability have been suggested in the literature for use in the optimal placement of actuators and sensors, respectively. A linear system is said to be controllable at time t_0 if there exists a $t_1 > t_0$ such that for any $x(t_0)$ and $x(t_1)$ there exists an input $u_{[t_0, t_1]}$ that will transfer the state $x(t_0)$ to the state $x(t_1)$ at time t_1 .¹¹ In linear, time-invariant systems, controllability can be measured from

the rank of the controllability grammian W_c , which is obtained from the solution of a Lyapunov equation

$$AW_c + W_c A^T = -BB^T \quad (17)$$

If the controllability grammian is full rank, then the system is said to be controllable. Furthermore, the range space of the columns of the controllability grammian represents the controllable modes of the system. One way to assess the rank of the controllability grammian is to examine its singular values, particularly its minimum singular value. The farther its minimum singular value is from zero, the more controllable the system will be. Therefore, singular values of the controllability grammian can be used as measures of controllability.

A linear system is said to be observable at time t_0 if there exists a $t_1 > t_0$ such that for any $x(t_0)$ at time t_0 the knowledge of the input $u_{[t_0, t_1]}$ and the output $y_{[t_0, t_1]}$ suffices to determine $x(t_0)$.¹¹ In linear, time-invariant systems, observability can be measured from the rank of the observability grammian W_o , which is obtained from the solution of a Lyapunov equation, i.e.,

$$A^T W_o + W_o A = -C^T C \quad (18)$$

The system is said to be observable if the observability grammian has a full rank. Moreover, the range space of the columns of the observability grammian represents the observable modes of the system. Similarly, the singular values of the observability grammian can be used as measures of observability of the system.

Although from the perspective of controllability and observability the problem of actuator and sensor placements appears to be disjoint, the joint consideration of these problems would have certain advantages. First, it would allow for joint and equal consideration of controllability and observability, i.e., modes that cannot be observed well are not considered in the placement of the actuators, or modes that are not controlled well are not considered in the placement of the sensors. Second, this joint consideration would ease the sensor-actuator placement problem when some or all of the sensor-actuator pairs need to be collocated, i.e., collocated rate feedbacks. In other words, this would remove the need for equality constraints, to guarantee collocated sensor and actuator locations, in the optimization. To achieve a joint and equal consideration of controllability and observability, the system is transformed into the balanced coordinates through a similarity transformation.¹⁷

$$\begin{aligned} \dot{z} &= Az + Bu \Rightarrow \dot{z} = P^{-1}AP\dot{z} + P^{-1}Bu \\ y &= Cz \Rightarrow y = CP\dot{z} \end{aligned} \quad (19)$$

Note that in a balanced realization, the controllability and observability grammians are equal and diagonal, i.e.,

$$H = \hat{W}_c = \hat{W}_o = \text{diag}[\sigma_1, \dots, \sigma_n] \quad (20)$$

The controllability or observability grammians in balanced coordinates are referred to as the Hankel matrix. The singular values of the Hankel matrix, $\sigma_1, \dots, \sigma_n$, include both measures of controllability and observability.

Optimization: Sensor-Actuator Placement

In the first criterion, an optimization is posed to obtain a set of optimal locations for the sensors and actuators which cause the transmission zeros of the system to move farther into the left-half plane. Considering only the n_z finite zeros of the system, the optimization problem may be posed as a nonlinear programming problem defined as

Minimize J :

$$J \equiv J_1 = \sum_{i=1}^{n_z} \frac{1}{|\text{Re}[z_i(x_1, \dots, x_{n_a})]|} \quad (21)$$

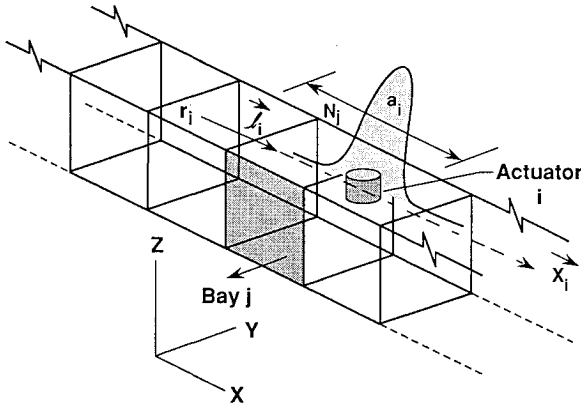


Fig. 1 Actuator force distribution on a typical truss section.

subject to

$$\begin{aligned} x_1^L &\leq x_1 \leq x_1^U \\ &\vdots \\ x_{n_a}^L &\leq x_{n_a} \leq x_{n_a}^U \end{aligned}$$

where z_1, \dots, z_{n_z} denote the n_z finite transmission zeros of the system, x_1, \dots, x_{n_a} are design variables representing the locations of the sensor-actuator pairs in their local coordinates, and $x_i^L, x_i^U, i = 1, \dots, n_a$ are the lower bound and upper bound values associated with the location of sensors and actuators. Here, the performance metric is the sum of the reciprocals of the absolute values of the real parts of the finite transmission zeros of the system and is mostly dominated by the zeros closest to the imaginary axis. As mentioned earlier, the transmission zeros are direct functions of the location of the sensors and actuators. Moreover, since the zeros are the solution of a generalized eigenvalue problem, they are continuous functions of the design variables x_1, \dots, x_{n_a} provided that the coefficient matrices of the generalized eigenvalue problem are continuous functions of x_1, \dots, x_{n_a} , which has been established by the functional approximations of the control forces and output measurements. The design variables x_1, \dots, x_{n_a} and their corresponding lower bound and upper bound values are defined in their local coordinate systems described by the reference points $r_i, i = 1, \dots, n_a$, and the direction vectors $l_i, i = 1, \dots, n_a$. One of the problems with optimizations that involve eigenvalues or zeros in their performance metric and/or constraint equations is the nondifferentiability brought about by the eigenvalues or zeros crossing each other as the design parameters change values. It is easy to observe from Eq. (21) that performance metric J_1 is devoid of this problem. Another issue of great importance is the continuity of the open-loop model. It is imperative to ensure that the reduced-order open-loop model obtained via modal truncation or modal cost analysis remains continuous as the design parameters change. One possible way of achieving this is to track the included modes. Another approach could be to make sure that there is enough separation between the mode with the largest frequency in the design model and the mode with the smallest frequency in the truncated model.

In the second criterion for sensor-actuator placement, the performance metric is chosen as the sum of the reciprocals of the singular values of the Hankel matrix, and the optimization problem is posed as a nonlinear programming problem as follows.

Minimize J :

$$J \equiv J_2 = \sum_{i=1}^{n_\sigma} \frac{1}{\sigma_i [H(x_1, \dots, x_{n_a})]} \quad (22)$$

subject to

$$\begin{aligned} x_1^L &\leq x_1 \leq x_1^U \\ &\vdots \\ x_{n_a}^L &\leq x_{n_a} \leq x_{n_a}^U \end{aligned}$$

where n_σ denotes the number of singular values of the Hankel matrix retained in Eq. (22). In this optimization, the location of the sensors and actuators are determined in order to increase a number singular values of the Hankel matrix, thereby increasing the effectiveness of the sensors and actuators as measured by the controllability and observability of the system. The reason for not including all of the singular values of the Hankel matrix in the performance metric is that some modes may not be practically controllable and/or observable for the allowable sensor-actuator configurations, i.e., their inclusion in Eq. (22) would hamper the optimization effort. It is also noted that the performance metric J_2 is mostly dominated by the smallest singular values.

The sensor-actuator placement algorithm may now be described as follows:

1) Based on the number of sensors and actuators to be used, divide the structure into several sections, and allocate actuators and sensors to each section by assigning appropriate reference points, direction vectors, and lower bounds and upper bounds. The choice on how to divide the structures or how to allocate the sensors and actuators to each section is to some degree based on engineering judgment.

2) Obtain the optimal locations for the sensors and actuators by solving the nonlinear programming problem of Eq. (21) or Eq. (22). It is noted that if the actuators or sensors have nonnegligible masses, i.e., the open-loop frequencies and mode shapes vary as the location of the sensors and actuators change, then the finite element model should be updated each time any of the design variables (sensor-actuator locations) change value.

This procedure describes a methodology for optimal sensor-actuator placement when the number of sensors and actuators is given. In some cases, however, the number of sensors and actuators to be used is not known and is considered to be a design parameter. One possible approach might then be to implement a multilevel optimization scheme, wherein integer programming, with the number of actuators and sensors allocated to each section as design variables, is used at the top level, followed by the described nonlinear programming approach to obtain the optimal locations of the sensors and actuators.

Numerical Results

The sensor-actuator placement algorithm is applied to the flexible space structure shown in Fig. 2. This structure represents a generic model of a space platform. The present finite element model is composed of a flexible bus, a 15-m antenna, a 7.5-m antenna, antenna support members, and 4468 kg of payload masses located within three bays of the bus. The antennas and their supports are assumed to be stiffer than the bus, and the antennas are locked at the gimbals. The structure has 98 nodes, at six degrees of freedom per node, resulting in

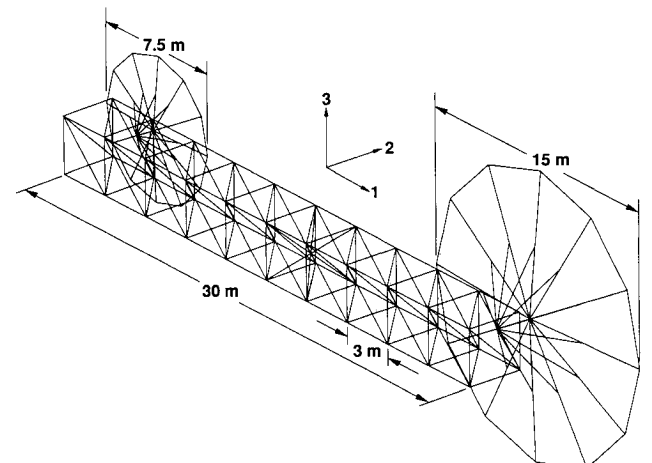


Fig. 2 Generic model of the geostationary platform.

a 588-order model. For the purpose of control design and analysis, however, a reduced-order model, which includes the three rotational rigid-body modes as well as the first ten flexible modes of the flexible structure, covering a bandwidth of 0–25 Hz, is generated. A modal damping ratio of 0.5% is assumed for each of the flexible modes. The resulting reduced-order model has 26 states.

The two criteria for sensor-actuator placement are employed to determine optimal locations for a set of six collocated sensor-actuator pairs consisting of torquers and attitude measurement sensors. First, the actuators are assumed to be ideal, i.e., there are no appreciable actuator dynamics. The reference points r_i , $i = 1, \dots, 6$, corresponding to each of the sensor-actuator pairs are chosen to coincide with point o , located 13.0 m from the small antenna. The sensors and actuators are assumed to be located in the middle of the bus cross section. The sensor-actuator pairs are allowed to be moved along the longitudinal axis of the bus, i.e., the direction vectors \bar{e}_i , $i = 1, \dots, 6$, are all chosen as $(1, 0, 0)$. The bus truss structure is divided into two sections, with three sensor-actuator pairs (acting along global X , Y , and Z) allocated to each section. The first section is from the support point of the small antenna to point o and the second section is from point o to the support point of the large antenna. The location of these six sensor-actuator pairs constitutes six design variables, i.e., design variables 1–3 correspond to the location of the three sensor-actuator pairs in section no. 1, and design variables 4–6 correspond to the location of the three sensor-actuator pairs in section no. 2. Using the first criterion, the cost function of Eq. (21), the optimization algorithm reduced the performance metric from an initial value of 53.5 to an optimal value of 40.2. The optimization was performed utilizing the Automated Design Synthesis (ADS) program.¹⁸ The solution of the generalized eigenvalue problem to obtain the transmission zeros of the system was computed using the EISPACK program.¹⁹ The initial values, the lower bounds and upper bounds, and the optimal values of the sensor-actuator locations, in local coordinates, are summarized in Table 1. The transmission zeros of the system for the initial and final sensor and actuator configurations are presented in Fig. 3. It appears from Fig. 3 that the transmission zeros closest to the imaginary axis are moved into the left-half plane, whereas those zeros farthest from the imaginary axis are moved toward the right-half plane, thus resulting in a more balanced dispersion of the zeros. Note that with this sensor-actuator configuration, the structure is more amenable to fast regulation and tracking. It is also noted that, for some transmission zeros, the increase in the absolute value of the real part is accompanied by an increase in their imaginary parts. This increase is of little consequence as long as the

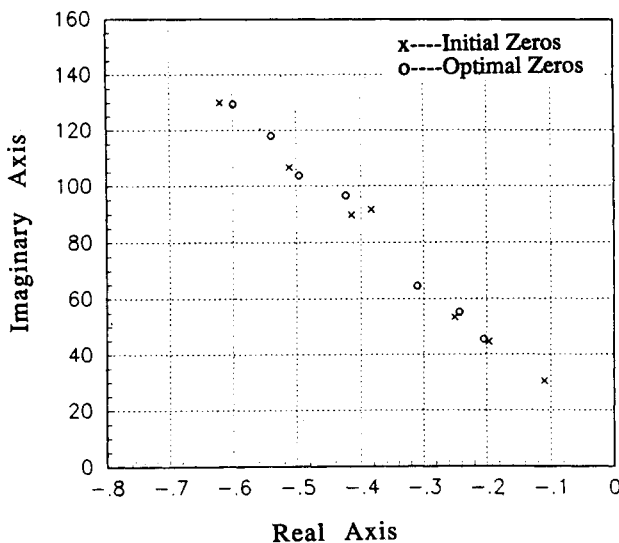


Fig. 3 Transmission zeros of the system.

Table 1 Optimization data and results for sensor-actuator pair locations

Design variable	Lower bound	Upper bound	Initial value	Final value
1	-13.3	1.00	-5.0	-4.53
2	-13.3	1.00	-5.0	-2.61
3	-13.3	1.00	-5.0	-4.24
4	1.00	16.3	6.0	12.16
5	1.00	16.3	6.0	14.51
6	1.00	16.3	6.0	7.04

Table 2 Optimization data and results for sensor-actuator pair locations

Design variable	Lower bound	Upper bound	Initial value	Final value
1	-13.3	1.00	-9.0	-13.3
2	-13.3	1.00	-9.0	-13.3
3	-13.3	1.00	-9.0	-13.3
4	1.00	16.3	10.0	4.52
5	1.00	16.3	10.0	7.51
6	1.00	16.3	10.0	16.3

open-loop poles and zeros are well separated, i.e., no pole-zero cancellation occurs.

The sensor-actuator placement problem is also performed following the second criterion [see Eq. (22)]. However, only the flexible modes are considered in the reduced-order model of the structure. Using the same reference point and direction vectors for the six sensor-actuator pairs, the optimization reduced the performance metric from an initial value of 1.45×10^5 to a final value of 0.72×10^5 . The initial values, the lower bounds and upper bounds, and the optimal values of the sensor-actuator locations are summarized in Table 2. The singular values of the Hankel matrix for the initial and final sensor and actuator configurations are shown in Table 3. Although all singular values increased, it seems that the largest relative increase in value are of the smallest singular values. This is because the performance metric given in Eq. (22) is mostly dominated by the smallest singular values. It should be mentioned that if some of the modes of the structure are practically uncontrollable and/or unobservable for the allowable sensor-actuator configurations, they should not be included in the design model since they tend to hamper the optimization process by totally dominating the performance metric.

Effect of Actuator Dynamics: To assess the effect of actuator dynamics on the optimal placement of sensors and actuators, each of the torquers is assumed to have second-order dynamics represented by the following transfer function

$$T_a(s) = \frac{\omega_a^2}{(s^2 + 2\zeta_a \omega_a s + \omega_a^2)} \quad (23)$$

A state-space realization of these dynamics, given by the actuator state matrix, input influence matrix, and output influence matrix, may be written as

$$A_{a_i} = \begin{bmatrix} 0 & 1 \\ -\omega_a^2 & -2\zeta_a \omega_a \end{bmatrix}, \quad B_i = \begin{bmatrix} 0 \\ \omega_a^2 \end{bmatrix}, \quad C_i = [1 \quad 0]$$

Since the dynamics of the actuators are not coupled, the state matrix for the actuator dynamics A_a is block diagonal with 2×2 matrices A_{a_i} on its diagonal. The actual bandwidth ω_a is chosen to coincide with the operational bandwidth of the system at 25 Hz, and the damping ratio ζ_a is assumed to be 0.2. The sensors and actuators are then placed following the second criterion for sensor-actuator placement [see Eq. (22)]. The op-

Table 3 Initial and optimal Hankel singular values

Initial singular values	Final singular values
0.14573×10^{-3}	0.20960×10^{-3}
0.14572×10^{-3}	0.20959×10^{-3}
0.45065×10^{-4}	0.58279×10^{-4}
0.45053×10^{-4}	0.58267×10^{-4}
0.26487×10^{-4}	0.35825×10^{-4}
0.26480×10^{-4}	0.35813×10^{-4}
0.23004×10^{-4}	0.27508×10^{-4}
0.23001×10^{-4}	0.27507×10^{-4}
0.20451×10^{-4}	0.27137×10^{-4}
0.20449×10^{-4}	0.27136×10^{-4}
0.19713×10^{-4}	0.25189×10^{-4}
0.19711×10^{-4}	0.25181×10^{-4}
0.14490×10^{-4}	0.24110×10^{-4}
0.14489×10^{-4}	0.24105×10^{-4}
0.11086×10^{-4}	0.23932×10^{-4}
0.11085×10^{-4}	0.23930×10^{-4}
0.10689×10^{-4}	0.17567×10^{-4}
0.10685×10^{-4}	0.17560×10^{-4}
0.38246×10^{-5}	0.16886×10^{-4}
0.38227×10^{-5}	0.16885×10^{-4}

Table 4 Optimization data and results for sensor-actuator pair locations

Design variable	Lower bound	Upper bound	Initial value	Final value
1	-13.3	1.00	-13.3	-13.3
2	-13.3	1.00	-13.3	-13.3
3	-13.3	1.00	-13.3	-13.3
4	1.00	16.3	4.52	4.52
5	1.00	16.3	7.51	10.51
6	1.00	16.3	16.3	13.48

Table 5 Initial and optimal Hankel singular values including actuator dynamics

Initial singular values	Final singular values
3.41927×10^{-4}	3.42090×10^{-4}
3.41139×10^{-4}	3.41299×10^{-4}
1.21579×10^{-4}	1.27336×10^{-4}
1.20471×10^{-4}	1.26020×10^{-4}
1.14222×10^{-4}	1.20762×10^{-4}
1.13689×10^{-4}	1.20339×10^{-4}
9.17746×10^{-5}	9.72375×10^{-5}
9.12370×10^{-5}	9.66675×10^{-5}
6.26615×10^{-5}	6.34505×10^{-5}
6.26400×10^{-5}	6.34281×10^{-5}
4.17281×10^{-5}	4.30490×10^{-5}
4.15890×10^{-5}	4.28943×10^{-5}
3.00355×10^{-5}	3.22139×10^{-5}
3.00233×10^{-5}	3.22029×10^{-5}
2.89281×10^{-5}	3.16436×10^{-5}
2.88902×10^{-5}	3.16077×10^{-5}
2.36964×10^{-5}	1.91985×10^{-5}
2.36100×10^{-5}	1.90803×10^{-5}
2.23144×10^{-5}	1.80150×10^{-5}
2.22604×10^{-5}	1.79446×10^{-5}
1.41071×10^{-5}	1.42166×10^{-5}
1.23585×10^{-5}	1.23948×10^{-5}
4.93019×10^{-6}	5.00990×10^{-6}
4.21581×10^{-6}	4.28705×10^{-6}
2.96059×10^{-6}	3.30389×10^{-6}
2.45747×10^{-6}	2.79709×10^{-6}
1.99959×10^{-6}	2.37011×10^{-6}
1.70059×10^{-6}	2.02476×10^{-6}
4.57518×10^{-7}	5.51022×10^{-7}
4.28515×10^{-7}	5.21338×10^{-7}
3.85710×10^{-7}	4.93449×10^{-7}
3.62704×10^{-7}	4.63538×10^{-7}

timization algorithm reduced the performance metric from an initial value 12.8×10^7 to a final value of 10.6×10^7 . The initial values, the lower bounds and upper bounds, and the optimal values of the sensor-actuator locations are given in Table 4. Note that the initial sensor-actuator configuration is chosen to be the optimal sensor-actuator configuration for the case without actuator dynamics. The initial and final singular values of the Hankel matrix are given in Table 5. Comparison of the singular values in Table 5 with those in Table 3 indicates that actuator dynamics result in a reduction of controllability, since the minimum singular value became smaller with actuator dynamics. Furthermore, the optimal sensor-actuator configurations given in Table 4 are quite different from those presented in Table 2, thus indicating that actuator dynamics can have substantial influence on the optimal positioning of sensors and actuators. It is expected that this influence becomes more pronounced as the actuator bandwidth decreases, and less profound as it moves farther from the operational bandwidth of the system. Moreover, the impact of actuator dynamics in the placement of sensors and actuators would be even more drastic if spillover is also considered when placing sensors and actuators. This is because modes in the spillover region are generally closer to the actuator bandwidth than modes in the operational bandwidth and, therefore, are more susceptible to the effects of actuator dynamics.

Concluding Remarks

An optimization-based approach for sensor and actuator placement in the control of flexible space structures has been outlined. In its first criterion, the approach utilizes the properties of the invariant transmission zeros, and optimally locates the sensors and actuators to move the transmission zeros of the system farther into the left-half plane. This is a feasible approach, particularly for fast optimal regulation and tracking problems, in view of the asymptotic trend of the closed-loop poles toward the zeros under high gains. In the second criterion, the sensors and actuators are optimally placed to increase the controllability and observability of the system by means of increasing the singular values of the Hankel matrix. Both criteria have been successfully applied to a large-order, flexible structure. Furthermore, the effect of actuator dynamics on the optimal placement of sensors and actuators has been investigated. It was shown that actuator dynamics can have considerable effect on the optimal locations of sensors and actuators, particularly when the actuator bandwidth is near the operational closed-loop bandwidth. Finally, the optimization-based nature of the approach is quite appealing because of its ability to both consider other performance metrics and impose design constraints, as well as its implementability in the controls-structures design environment.

References

- Chen, W. H., and Seinfeld, J. H., "Optimal Location of Process Measurements," *International Journal of Control*, Vol. 21, No. 6, 1975, pp. 1003-1014.
- Skelton, R. E., and Chiu, D., "Optimal Selection of Inputs and Outputs in Linear Stochastic Systems," *Journal of the Astronautical Sciences*, Vol. XXXI, No. 3, July-Sept. 1983, pp. 399-414.
- Horta, L. G., and Juang, J.-N., "A Sequential Linear Optimization Approach for Controller Design," *Journal of Guidance, Control, and Dynamics*, Vol. 9, No. 6, 1986, pp. 699-703.
- Hughes, P. C., and Skelton, R. E., "Controllability and Observability for Flexible Spacecraft," *Journal of Guidance and Control*, Vol. 3, No. 5, 1980, pp. 452-459.
- Longman, R. W., and Alfriend, K. T., "Energy Optimal Degree of Controllability and Observability for Regulator and Maneuver Problems," *Proceedings of the Sixteenth Annual Conference on Information Sciences and Systems* (Princeton, NJ), March 1982, pp. 633-638.
- Lindberg, R. E., and Longman, R. W., "Optimization of Actuator Placement via Degree of Controllability Criteria Including Spillover Considerations," AIAA Paper 82-1435; see also AIAA/AAS Astrodynamics Conference, San Diego, CA, Aug. 9-11, 1982.
- Longman, R. W., and Horta, L. G., "Actuator Placement by Degree of Controllability Including the Effect of Actuator Mass,"

Proceedings of the Seventh VPI&SU/AIAA Symposium on Dynamics and Control of Large Flexible Spacecraft (Blacksburg, VA), May 1989, pp. 245-260.

⁸Maghami, P. G., and Joshi, S. M., "Sensor/Actuator Placement for Flexible Space Structures," *Proceedings of the 1990 American Control Conference* (San Diego, CA), Inst. of Electrical and Electronics Engineers, Piscataway, NJ, May 1990, pp. 1941-1948.

⁹Lim, K. B., "A Method for Optimal Actuator and Sensor Placement for Large Flexible Structures," *Journal of Guidance, Control, and Dynamics*, Vol. 15, No. 1, 1992, pp. 49-57.

¹⁰Kwakernaak, H., "Asymptotic Root Loci of Multivariable Linear Optimal Regulators," *IEEE Transactions on Automatic Control*, Vol. 21, June 1976, pp. 378-382.

¹¹Kouvaritakis, B., "The Optimal Root Loci of Linear Multivariable Systems," *International Journal of Control*, Vol. 28, July 1978, 1978, pp. 33-62.

¹²Williams, T., "Transmission-Zero Bounds for Large Space Structures, with Applications," *Journal of Guidance, Control, and Dynamics*, Vol. 12, No. 1, 1989, pp. 33-38.

¹³Lighthill, M. J., *Fourier Analysis and Generalized Functions*,

Cambridge University Press, New York, 1964, Chap. 2.

¹⁴Kwakernaak, H., and Sivan, R., *Linear Optimal Control Systems*, Wiley-Interscience, New York, 1972, Chap. 3.

¹⁵Emami-Naeini, A., and Van Dooren, P., "Computation of Zeros of Linear Multivariable Systems," *Automatica*, Vol. 18, No. 4, 1982, pp. 415-430.

¹⁶Williams, T., "Computing the Transmission Zeros of Large Space Structures," *IEEE Transactions on Automatic Control*, Vol. 34, No. 1, 1989, pp. 92-94.

¹⁷Moore, B. C., "Principal Component Analysis in Linear Systems: Controllability, Observability, and Model Reduction," *IEEE Transactions on Automatic Control*, Vol. AC-26, No. 1, Feb. 1981, pp. 17-32.

¹⁸Vanderplaats, G. N., "ADS—A Fortran Program for Automated Design Synthesis—Version 1.10," NASA CR 177985, NASA Langley Research Center, Hampton, VA, Sept. 1985.

¹⁹Garbow, B. S., Boyle, J. M., Dongarra, J. J., and Moler, C. B., *Matrix Eigensystem Routines—EISPACK Guide Extension*, Lecture Notes in Computer Science 51, edited by G. Goos and J. Hartmanis, Springer-Verlag, Berlin, 1977.

AIAA Education Series

Nonlinear Analysis of Shell Structures

A.N. Palazotto and S.T. Dennis

The increasing use of composite materials requires a better understanding of the behavior of laminated plates and shells for which large displacements and rotations, as well as, shear deformations, must be included in the analysis. Since linear theories of shells and plates are no longer adequate for the analysis and design of composite structures, more refined theories are now used for such structures.

This new text develops in a systematic manner the overall concepts of the nonlinear analysis of shell structures. The authors start with a survey of theories for the analysis of plates and shells with small

deflections and then lead to the theory of shells undergoing large deflections and rotations applicable to elastic laminated anisotropic materials. Subsequent chapters are devoted to the finite element solutions and include test case comparisons.

The book is intended for graduate engineering students and stress analysts in aerospace, civil, or mechanical engineering.

1992, 300 pp, illus, Hardback, ISBN 1-56347-033-0, AIAA Members \$47.95, Nonmembers \$61.95, Order #:33-0 (830)

Place your order today! Call 1-800/682-AIAA



American Institute of Aeronautics and Astronautics

Publications Customer Service, 9 Jay Gould Ct., P.O. Box 753, Waldorf, MD 20604
FAX 301/843-0159 Phone 1-800/682-2422 9 a.m. - 5 p.m. Eastern

Sales Tax: CA residents, 8.25%; DC, 6%. For shipping and handling add \$4.75 for 1-4 books (call for rates for higher quantities). Orders under \$100.00 must be prepaid. Foreign orders must be prepaid and include a \$20.00 postal surcharge. Please allow 4 weeks for delivery. Prices are subject to change without notice. Returns will be accepted within 30 days.